






RESEARCH PAPER

Carbonic anhydrase II does not regulate nitrite-dependent nitric oxide formation and vasodilation

Ling Wang^{1,2}  | Courtney E. Sparacino-Watkins^{1,2}  | Jun Wang³ |
 Nadeem Wajih⁴ | Paul Varano¹ | Qinzi Xu¹  | Eric Cecco¹ | Jesús Tejero^{1,2}  |
 Manoocher Soleimani⁶ | Daniel B. Kim-Shapiro^{4,5} | Mark T. Gladwin^{1,2} 

¹Pittsburgh Heart, Lung, Blood and Vascular Medicine Institute, University of Pittsburgh, Pittsburgh, Pennsylvania

²Division of Pulmonary, Allergy and Critical Care Medicine, Department of Medicine, University of Pittsburgh, Pittsburgh, Pennsylvania

³Hubei University of Technology, Wuhan, P. R. China

⁴Department of Physics, Wake Forest University, Winston-Salem, North Carolina

⁵Translational Science Center, Wake Forest University, Winston-Salem, North Carolina

⁶Department of Medicine, University of Cincinnati, Cincinnati, Ohio

Correspondence

Ling Wang, Pittsburgh Heart, Lung, Blood and Vascular Medicine Institute, University of Pittsburgh, Pittsburgh, PA.
 Email: lingwang@pitt.edu

Courtney Sparacino-Watkins, Division of Pulmonary, Allergy and Critical Care Medicine, Department of Medicine, University of Pittsburgh, Pittsburgh, PA.
 Email: cew35@pitt.edu

Funding information

National Heart, Lung, and Blood Institute, Grant/Award Numbers: P01 HL103455, R01 HL098032, R01 HL125886, R37HL058091, T32 HL110849; The Burroughs Wellcome Foundation; The Hemophilia Center of Western Pennsylvania; The Institute for Transfusion Medicine; NIH, Grant/Award Numbers: 4R37HL058091-20, 5T32HL110849-08, 5P01HL103455-09, 2R01HL125886-05, 5R01HL098032-11; UPCI Cancer Biomarkers Facility, Grant/Award Number: P30CA047904

Background and purpose: Although it has been reported that bovine carbonic anhydrase CAII is capable of generating NO from nitrite, the function and mechanism of CAII in nitrite-dependent NO formation and vascular responses remain controversial. We tested the hypothesis that CAII catalyses NO formation from nitrite and contributes to nitrite-dependent inhibition of platelet activation and vasodilation.

Experiment approach: The role of CAII in enzymatic NO generation was investigated by measuring NO formation from the reaction of isolated human and bovine CAII with nitrite using NO photolysis-chemiluminescence. A CAII-deficient mouse model was used to determine the role of CAII in red blood cell mediated nitrite reduction and vasodilation.

Key results: We found that the commercially available purified bovine CAII exhibited limited and non-enzymatic NO-generating reactivity in the presence of nitrite with or without addition of the CA inhibitor dorzolamide; the NO formation was eliminated with purification of the enzyme. There was no significant detectable NO production from the reaction of nitrite with recombinant human CAII. Using a CAII-deficient mouse model, there were no measurable changes in nitrite-dependent vasodilation in isolated aorta rings and in vivo in CAII^{-/-}, CAII^{+/-}, and wild-type mice. Moreover, deletion of the CAII gene in mice did not block nitrite reduction by red blood cells and the nitrite-NO-dependent inhibition of platelet activation.

Conclusion and implications: These studies suggest that human, bovine and mouse CAII are not responsible for nitrite-dependent NO formation in red blood cells, aorta, or the systemic circulation.

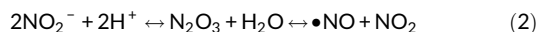
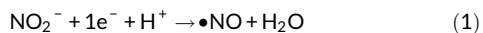
Abbreviations: AO, aldehyde oxidase; CA, carbonic anhydrase; Cu-NiR, copper nitrite reductase; Hct, haematocrit; IMAC, immobilized metal affinity chromatography; KO, knockout; LC-MS/MS, liquid chromatography tandem MS; mARC, mitochondrial amidoxime reducing component; NOA, nitric oxide analyser; *p*-NPA, *para*-nitrophenyl acetate; *p*-NP, *para*-nitrophenyl; c-PTIO, 2-(4-Carboxyphenyl)-4,4,5,5-tetramethylimidazole-1-oxyl-3-oxide; RSNO, S-nitrosothiol; SNP, sodium nitroprusside; SO, sulfite oxidase; WT, wild type; XO, xanthine oxidoreductase.

Ling Wang and Courtney Sparacino-Watkins should be considered joint first author.

1 | INTRODUCTION

In mammalian systems, NO is a critical signalling molecule. It is now appreciated that nitrite (NO₂⁻) functions as an endocrine and paracrine reservoir of NO, present in plasma and tissues. Accumulating evidence suggests that nitrate and nitrite metabolism occurs in blood and tissues to form NO and other bioactive nitrogen oxides, which regulates important functions such as hypoxic vasodilation, and cytoprotection (Gladwin et al., 2006; Lundberg et al., 2009; Lundberg, Weitzberg, & Gladwin, 2008). This physiological and hypoxic nitrite-dependent NO pathway complements the traditional normoxic L-arginine-NOS-NO pathway, which relies on oxygen and L-arginine as substrates (Lundberg et al., 2009; Shiva, 2013).

Many enzymatic sources of nitrite-dependent NO formation have been reported in mammals, although the enzyme catalyzing such NO formation in vivo depends on several factors including location (tissue, cell, and organelle), environment (pH or oxygen content), and physiological or pathological status. Two chemical reaction pathways, nitrite reduction and nitrite anhydrase, have been proposed for the generation of NO from nitrite (Equations (1) and (2); Kim-Shapiro & Gladwin, 2014).



Most vertebrate nitrite-dependent NO-generating enzymes act as nitrite reductases (Equation (1)), although nitrite anhydrase catalysed reactions (Equation (2)) have been reported as well. Many haem-containing proteins with nitrite reductase activities have been described, including haemoglobin (Huang et al., 2005), myoglobin (Shiva et al., 2007), neuroglobin (Tiso et al., 2011), cytoglobin (Li, Hemann, Abdelghany, El-Mahdy, & Zweier, 2012), and globin X (Corti et al., 2016). All four molybdenum (Mo)-containing enzymes function as nitrite reductases, which are **xanthine oxidoreductase (XO)**; Li, Samouilov, Liu, & Zweier, 2001), aldehyde oxidase (AO; Li, Kundu, & Zweier, 2009), sulfite oxidase (SO; Wang et al., 2015), and mitochondrial amidoxime reducing component (mARC; Sparacino-Watkins et al., 2014). Haemoglobin (Basu et al., 2007), nitrophorin (He & Knipp, 2009), and the zinc-containing **carbonic anhydrase (CA) II** (Aamand et al., 2009b) have been reported to exhibit nitrite anhydrase activities. However, the role of CAII in nitrite-dependent NO formation remains controversial as a number of studies have been unable to detect changes in measured NO formation from nitrite with red blood cells (Liu et al., 2015) and in vivo after treatment with CA inhibitors (Andring et al., 2018; Pickerodt et al., 2018; Zinke, Hanff, Böhmer, Supuran, & Tsikas, 2016).

Since its discovery in the 1930s, CA has been known for its substrate specificity, selectively binding carbon dioxide (CO₂) and bicarbonate (HCO₃⁻), which catalyses the rapid interconversion of CO₂ and water to HCO₃⁻ (Equation (3)). Classically, CA acts as a metabolic enzyme that regulates intracellular pH levels and CO₂ transport (Lindskog, 1997; Silverman & Lindskog, 1988). So far, 13 catalytically

What is already known

- Several mammalian metalloenzymes can catalyse nitrite-dependent synthesis of nitric oxide (NO).
- The contribution of carbonic anhydrase II to nitrite-dependent synthesis of NO remains controversial.

What does this study add

- Purified bovine or human recombinant carbonic anhydrase II did not generate NO from nitrite.
- Nitrite-dependent vasodilation in vitro or in vivo, was unchanged in mice lacking carbonic anhydrase II.

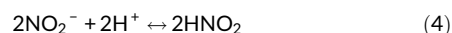
What is the clinical significance

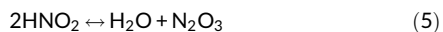
- Elucidation of nitrite reduction pathways that produce the vasodilator NO is critical to vascular physiology.
- Vasodilation by carbonic anhydrase inhibitors is unlikely to be related to NO formation from nitrite.

active **CA isoforms** have been reported in mammals, which differ in subcellular location (cytosolic, membrane, and extracellular), tissue expression patterns, catalytic competency, and physiological function (Supuran, 2008). The well-characterized cytosolic isoform, CAII, is highly expressed in erythrocytes and specifically important for CO₂ transportation and excretion (Swenson & Maren, 1978). Inhibitors of CAII, such as monovalent anions, sulfonates, and sulfonamides have important pharmacological implications and have been the focus of multiple investigations.



In 2009, Aamand and colleagues reported that CAII not only bound to nitrite, a known anionic carbonic anhydrase inhibitor (Innocenti, Zimmerman, Ferry, Scozzafava, & Supuran, 2004; Nielsen & Fago, 2015), but also converted nitrite to NO (Aamand et al., 2009b). The proposed mechanism of nitrite anhydrase resembles the CO₂ anhydrase activity (Equation (3); Innocenti, Zimmerman, et al., 2004). First nitrite binds to proton to make nitrous acid (Equation (4)), which reacts with a second nitrite to form water and N₂O₃ (Equation (5)). Generated N₂O₃ is then dissociated into NO and NO₂ (Equation (6)). Later work by Hanff et al. (2018) supports a role for CA in generation of HNO₂ and N₂O₃, but not NO production. Although the concept of catalytic nitrite dehydration to form N₂O₃ is intriguing and suggests a dual function for CAII in erythrocytes, solid biological evidence is lacking, and the CAII-nitrite-NO pathway has yet to be validated in vivo.





The possible roles of CA in nitrite metabolism in the kidney and vasculature are a matter of active research (Chobanyan-Jürgens et al., 2012; Zinke et al., 2016). However, it is pertinent to mention that studies by Hanff et al. (2016) indicate that neither CAII nor CAIV directly generates NO from nitrite. Interestingly, the authors found that CAII was able to stimulate cGMP production in the presence of nitrite using either purified recombinant soluble guanylyl cyclase or washed human platelets, an activity linked to S-nitrosothiol (RSNO) production by CAII in the presence of cysteine (Hanff et al., 2016).

In order to fully address this controversy, we performed additional studies to determine if CAII mediates NO generation from nitrite, *in vitro* and *in vivo*. We specifically tested the hypothesis that CAII mediates NO formation from nitrite and regulates nitrite-dependent inhibition of platelet activation and vasodilation. We investigated the role of human CAII in enzymic nitrite-dependent NO formation with NO detection by gas phase chemiluminescence, as the human CAII reactivity with nitrite has not been reported using this method. We also performed platelet activation assays in the presence of red blood cells, and used a global CAII-deficient mouse model, to identify whether CAII mediates nitrite-dependent platelet inhibition and both *ex vivo* and *in vivo* vasodilation.

2 | METHODS

2.1 | Animals

All animal care and experimental studies were performed using protocols approved by the Institutional Animal Care and Use Committee at the University of Pittsburgh (Protocol number 16099210) and in accordance with National Institutes of Health guidelines. CAII-deficient (CAII^{-/-}) mice were produced by mutagenesis as previously reported (Lewis, Erickson, Barnett, Venta, & Tashian, 1988). All CAII^{-/-} mice and their heterozygous and wild-type litter mates were bred and maintained in University of Pittsburgh animal facility at a controlled temperature of 22–23°C and a humidity of 50–60% with a 12-hr light/12-hr dark cycle. Animals were adapted to the standard housing conditions for 1 week before experiments. Animal studies are reported in compliance with the ARRIVE guidelines (Kilkenny, Browne, Cuthill, Emerson, & Altman, 2010; McGrath & Lilley, 2015) and with the recommendations made by the British Journal of Pharmacology.

A total of 87 adult male mice including CAII^{-/-} mice and their heterozygous and wild-type littermates ($n = 29$ respectively, 10–12 weeks, 26–32 g) were used in the studies. All three genotype groups had equal sample sizes. As this was not a therapeutic study, randomization of animals was not performed. The surgical operator and data analysis were blinded to the experimental groups. No animals were excluded from statistical analysis. Animals were killed by

the application of isoflurane as an anaesthetic (5%, balanced with oxygen) using a precision vaporizer followed by cervical dislocation.

2.2 | Preparation of isolated CAII enzymes

Bovine CAII isolated from erythrocytes was purchased from Sigma. The lyophilized protein was dissolved in 10-mM phosphate buffer at pH 7.2. Recombinant human CAII enzyme was isolated from *Escherichia coli* using standard procedures. The human CAII pET11 Amp^R expression plasmid was obtained from David Silverman (Fisher et al., 2005; Tu, Silverman, Forsman, Jonsson, & Lindskog, 1989). DNA sequencing, with universal sequencing primers (T7 binding forward primer and M13 binding reverse primer) was used to verify that the entire 783 bp human CAII gene was maintained in the pET11 plasmid. The amplified DNA sequence was aligned with the human CAII mRNA reference sequence (NM_000067.2) to verify that the 260 amino acid human CAII protein sequence (NP_000058.1) was encoded in the expression plasmid. *E. coli* strain SoluBI21 was transformed with the human CAII pET11 expression plasmid and grown in zinc sulphate (1 mM) supplemented Lysogeny broth (LB) media with ampicillin (100 mg·mL⁻¹) prior to expression induction with isopropyl β-D-1-thiogalactopyranoside (100 mM).

Immobilized metal affinity chromatography (IMAC) was used to isolate human and bovine CAII. Native CAII enzyme can be purified in a one-step chromatographic separation using IMAC resin without the addition of a poly-histidine affinity tag (Banerjee, Swanson, Mallik, & Srivastava, 2004). It is thought that the close proximity of three histidine residues in the CAII active site mimics the poly-histidine affinity tag to facilitate IMAC binding (Banerjee et al., 2004). While CAII binds to zinc-, copper-, or nickel-loaded IMAC resins and can be isolated with little (less than 5%) metal leaching (GE Healthcare Bio-Sciences, Sweden, Application note 28-4044-80 AA), zinc was selected to minimize exposure to other metals. Briefly, the IMAC sepharose resin (GE) was charged with Zn²⁺ using 20-mM sodium phosphate buffer with 500-mM NaCl at pH 7.4. The lyophilized bovine CAII protein was dissolved in 10-mM phosphate buffer at pH 7.2 prior to application to the column. For the human CAII, clarified *E. coli* lysate was loaded onto the IMAC. After washing unbound proteins from the resin, elution was achieved using a stepwise introduction of a low pH buffer (20-mM sodium acetate, 500-mM NaCl at pH 4.5). Immediately after fraction collection, the acidic pH was neutralized by the addition of 100-mM sodium phosphate at pH 8. Centrifugal concentrating devices (Amicon) were used for buffer exchange, salt removal, and concentration prior to use.

Next, CAII enzyme activity was measured using the *para*-nitrophenyl acetate (*p*-NPA) activity assay (Pocker & Stone, 1967). Briefly, CAII was incubated with 400-μM *p*-NPA in 100-mM phosphate buffer at pH 7.4. The rate of *p*-NPA hydrolysis to *p*-nitrophenol was measured by following the appearance of the 405-nm absorbance band over time in a Cary UV-VIS spectrophotometer. The background (non-enzymic) rate of *p*-NPA hydrolysis was measured prior to enzyme injection in each run and then subtracted from the enzymic rate.

2.3 | Mass spectrometry

Proteolytic peptides from in-gel trypsin digestion were analysed by a nanoflow reverse-phased liquid chromatography tandem MS (LC-MS/MS). In-gel trypsin digestion, carried out as previously described (Shevchenko, Tomas, Havlis, Olsen, & Mann, 2006), was chosen to facilitate extraction of discrete protein bands separated with SDS-PAGE and stained with Coomassie dye. In this method, immobilized protein bands were manually extracted from the acrylamide matrix using a razor, chemically treated to remove dye and minimize acrylamide matrix, and then digested with trypsin proteases. Tryptic peptides were loaded onto a C18 column (PicoChip™ column packed with 10.5-cm Reprosil C18 3- μ m 120-Å chromatography media with a 75- μ m ID column and a 15- μ m tip, New Objective, Inc., Woburn, MA) using a Dionex HPLC system and injected into a linear ion trap MS (LTQ-XL, ThermoFisher Scientific) through electrospray.

MS/MS spectra were searched using MASCOT search engine (Version 2.4.0, Matrix Science Ltd.) against the UniProt bovine proteome database. The following modifications were used: static modification of cysteine (carboxyamidomethylation, +57.05 Da) and variable modification of methionine (oxidation, +15.99 Da). The mass tolerance was set at 1.4 Da for the precursor ions and 0.8 Da for the fragment ions. Peptide identifications were filtered using PeptideProphet™ and ProteinProphet® algorithms with a protein threshold cut-off of 99% and peptide threshold cut-off of 90% implemented in Scaffold™ (Proteome Software, Portland, Oregon, USA).

2.4 | Determination of NO formation by NO photolysis-chemiluminescence

Kinetic NO formation from nitrite was measured using NO photolysis-chemiluminescence in a Sievers 280i NO analyser (NOA, from GE Analytical Instruments) as described previously (Sparacino-Watkins et al., 2014). A NOA was used for all kinetic measurements of NO formation, because NO chemiluminescence has unmatched sensitivity, is selective for NO, and is a standard method used to characterize nitrite-dependent NOSs, such as XO (Li et al., 2001), mARC (Sparacino-Watkins et al., 2014), SO (Wang et al., 2015), AO (Li et al., 2009), and CAII (Aamand et al., 2009b).

Liquid software (Version 3) was used to monitor and collect data. Enzyme assays were performed in 10-mM phosphate buffer at pH 7.2 and 37°C under anaerobic conditions unless otherwise noted. Buffers were purged with argon to remove oxygen before the addition of enzyme. Reagents and enzymes were injected into the reaction vessel through butyl rubber septa using a gas-tight Hamilton syringe. For each reaction, data were collected for at least 10 min. Raw data from the NOA were transferred into Origin Lab software (Version 8.6) to calculate rates of NO formation. The raw data were transformed using an experimentally determined instrument calibration equation, as described previously (MacArthur, Shiva, & Gladwin, 2007). Briefly, known amounts of nitrite were injected into the purge vessel containing an acidified tri-iodine solution. Instantaneous equimolar

conversion of nitrite to NO generated peaks, these peaks were then integrated. Next, the AUC (mV·min) data were plotted against the amount of nitrite injected (pmol) to determine the linear relationship between AUC and NO. The slope (e.g., 0.139 mV·min·pmol⁻¹ of NO) generated with nitrite standard calibration was then used to convert raw electronic signal (mV) data to NO production rate (pmol·NO·min⁻¹) for the enzymic experiments, as the NOA rapidly measures NO production rate over time. The maximum peak height, produced approximately 30 s after CAII enzyme injection, was averaged for 10 s and reported as the NO production rate. The NO production rate was then divided by CAII enzyme concentration to yield a normalized rate (pmol·NO·min⁻¹·mg⁻¹ of CAII).

2.5 | Preparation of red blood cell ghosts

The red blood cell ghosts were prepared from freshly collected mouse blood. Fresh blood was centrifuged at 4°C, 1,500× g for 10 min to remove the buffy coat and RBC pellets were washed with PBS twice. The washed RBC pellets were suspended in 10 volumes of a ghosting buffer (10 mM Na₂HPO₄, 30 mM NaN₃, and 1 mM EDTA, pH 8) with Complete Protease Inhibitor Cocktail (1 μ g·ml⁻¹; Roche Applied Science) and incubated at 4°C with rotation for 30 min, then centrifuged at 4°C, 1,500× g for 15 min to remove supernatant. The pellet ghosts were re-suspended with ghosting buffer and incubated at 4°C with rotation for 30 min for three more times and were then ready to use.

2.6 | Western blotting analysis

Mouse tissue samples (kidney, liver, heart, lung, aorta, and red blood cell ghosts) were lysed in ice-cold lysis buffer (20 mM Tris pH 7.5, 150 mM NaCl, 1 mM EDTA, 1 mM EGTA, 1% Triton X-100, 2.5 μ M Na-pyrophosphate, 1 mM β -glycerophosphate, 1 mM Na₃VO₄, 1 mM phenylmethylsulfonyl fluoride, and Complete Protease Inhibitor Cocktail, 1 μ g·ml⁻¹). Protein lysates (20- μ g total protein) were separated on a NuPAGE™ 4–12% SDS Bis-Tris protein gel (Invitrogen, #NP0323) under reducing conditions, followed by electrotransfer to a nitrocellulose membrane (0.45 μ m, Bio-Rad, #1620115). After blocking with blocking buffer (SuperBlock™ TBS Blocking Buffer, Thermo Fisher Scientific, #37537) for 2 hr at room temperature, the membranes were probed with rabbit anti-CAII monoclonal antibody (1:1,000 dilution, Abcam, #ab124687, RRID: AB_10972000), mouse anti-GAPDH monoclonal antibody (1:1,000 dilution, Santa Cruz Biotechnology, sc-32233, RRID: AB_627679), and mouse anti- β -actin monoclonal antibody (1:1,000 dilution, Sigma-Aldrich, #A2228, RRID: AB_476697) in blocking buffer supplemented with 0.1% (v/v) Tween 20 at 4°C overnight and then washed three times with TBS supplemented with 0.1% (v/v) Tween 20 (TBS-T). Blots were incubated with HRP-conjugated secondary antibodies (goat anti-rabbit IgG, 1:10,000 dilution, Abcam, ab6721, RRID: AB_955447; rabbit anti-mouse IgG, 1:10,000 dilution, Abcam, ab97046, RRID: AB_10680920) in blocking buffer supplemented with 0.1% (v/v) Tween 20 for 1 hr at room temperature.

Protein bands were detected by using Clarity Western ECL Substrate (Bio-Rad, #1705060) and ChemiDoc Imaging System (Bio-Rad, USA). The experimental detail provided conforms with BJP Guidelines (Alexander et al., 2018).

2.7 | Aortic ring myography

Thoracic aortas of mice were cleared of adherent adipose tissue and cut into 2-mm-long rings. Arterial segments were mounted on myograph pins (Danish Myo Technology, Atlanta, GA) in 5-ml incubation buffer maintained at 37°C, pH 7.4, gassed with 95% O₂ and 5% CO₂, and brought to an optimal resting tension. Rings were gradually stretched to 500 mg and allowed to equilibrate for 30 min. Viability of the vessels was ascertained by a contractile response to 60-mM potassium chloride. After washing and further equilibration, the rings were contracted with 0.1 μM phenylephrine (Sigma-Aldrich). After stabilization, relaxation was assessed by the cumulative addition of sodium nitrite (0.1 μM–1 mM) or sodium nitroprusside (SNP, 0.1 nM–1 μM). Vasodilator responses were expressed as a percentage of relaxation of phenylephrine-induced pre-constriction (%relaxation).

2.8 | Platelet activation assay

Inhibition of platelet activation by nitrite in the presence of red blood cells was examined as previously published (Liu et al., 2015). Blood was drawn into heparinized tubes from CAII^{-/-}, CAII^{+/-}, and wild-type mice. Red blood cells were washed by centrifugation (1,000× g for 10 min) in PBS at pH 7.4, pH 6.8, or pH 6.5 at least three times or until the supernatants were clear. After the final wash, red blood cells were re-suspended at 70% haematocrit (Hct). All the experiments were conducted within 24 hr after the blood samples were drawn. Deoxygenated washed red blood cells were prepared by blowing nitrogen gas across the suspension with gentle rocking at room temperature for 30 min. Platelet rich plasma (PRP) was prepared by centrifuging whole blood at 120× g for 15 min at room temperature. PRP was removed by plastic disposable pipettes without disturbing the buffy coat and was stored in polypropylene tubes for use within 2 hr. All necessary materials were placed inside an air-tight glove bag filled with nitrogen gas. PRP was diluted 1:7 in deoxygenated PBS, pH 7.4. Nitrite (10 μM) was added as indicated and washed RBCs were added to 15% Hct, and the mixtures were incubated at 37°C for 5 min. After 5 min, 1-μM ADP was added to initiate activation and allowed to incubate for 6 min at 37°C. Samples were then incubated with FITC labelled PAC-1 and Per-CP labelled CD61 antibodies (BD Bioscience) for 15 min in the dark and diluted 1:50 in 1% formaldehyde to stop the reaction. The average RBC oxygen saturation was 20%, as determined by absorbance spectroscopy. A BD Biosciences FACSCalibur flow cytometer and Cell Quest Pro software were used for data collection and analysis. The activation threshold was set, so 99% of baseline platelets were beneath the threshold.

2.9 | In vivo arterial blood pressure measurements

Mice were anaesthetized using 2% isoflurane gas, and a tracheal tube was inserted followed by cannulation of right jugular vein and left carotid artery. Ventilation was initiated after the surgery with a volume-controlled ventilator (MiniVent, Type 845; Hugo Sachs). Air was administered (21% oxygen) with 1.5% isoflurane at tidal volumes of 228–270 μl (8.8 μl·g⁻¹ weight) and respiratory frequencies of 175 BPM. Arterial blood pressure was monitored and recorded (DATAQ instruments) through a catheter in the carotid artery. An intravenous catheter was placed in the jugular vein and used for sodium nitrite or PBS infusions using a syringe pump. Nitrite (30–2,500 nmol) in PBS was infused over 5 min with a rate of 12 μl·min⁻¹ to give a 75-μl infusion (50 μl delivered to animals, 20 μl dead space in catheter). Arterial blood pressure and heart rate signals were processed using Labchart software (ADInstruments Ltd.).

2.10 | Data and statistical analysis

The data and statistical analysis comply with the recommendations of the *British Journal of Pharmacology* on experimental design and analysis in pharmacology (Curtis et al., 2018). All groups were assigned equal sample sizes representing number of independent values, and statistical analysis was carried out using these independent values. Data were presented as means ± SEM or means ± SD as indicated in the figure legends. Vasodilator responses were expressed as a percentage of relaxation of phenylephrine-induced pre-constriction. Group sizes were selected based on our previous experience of the variability of the measurements without carrying out a formal power analysis. Statistical analysis was undertaken only for studies where each group size was at least $n = 5$. Any data with small group sizes ($n < 5$) were not subjected to statistical analysis. No outliers were excluded from statistical analysis. Data were analysed by unpaired Student's *t* test or one-way ANOVA, unless indicated otherwise. Two-way ANOVA with repeated measures was performed to determine the effects of nitrite on arterial blood pressure. Post-tests were run only if *F* achieved $P < .05$ and there was no significant variance in homogeneity. Statistical analyses were performed using GraphPad Prism software Version 6.0. $P < .05$ was considered significant.

2.11 | Materials

All chemicals were purchased from Sigma-Aldrich Inc. (St. Louis, MO, USA) unless otherwise noted.

2.12 | Nomenclature of targets and ligands

Key protein targets and ligands in this article are hyperlinked to corresponding entries in <http://www.guidetopharmacology.org>, the common portal for data from the IUPHAR/BPS Guide to

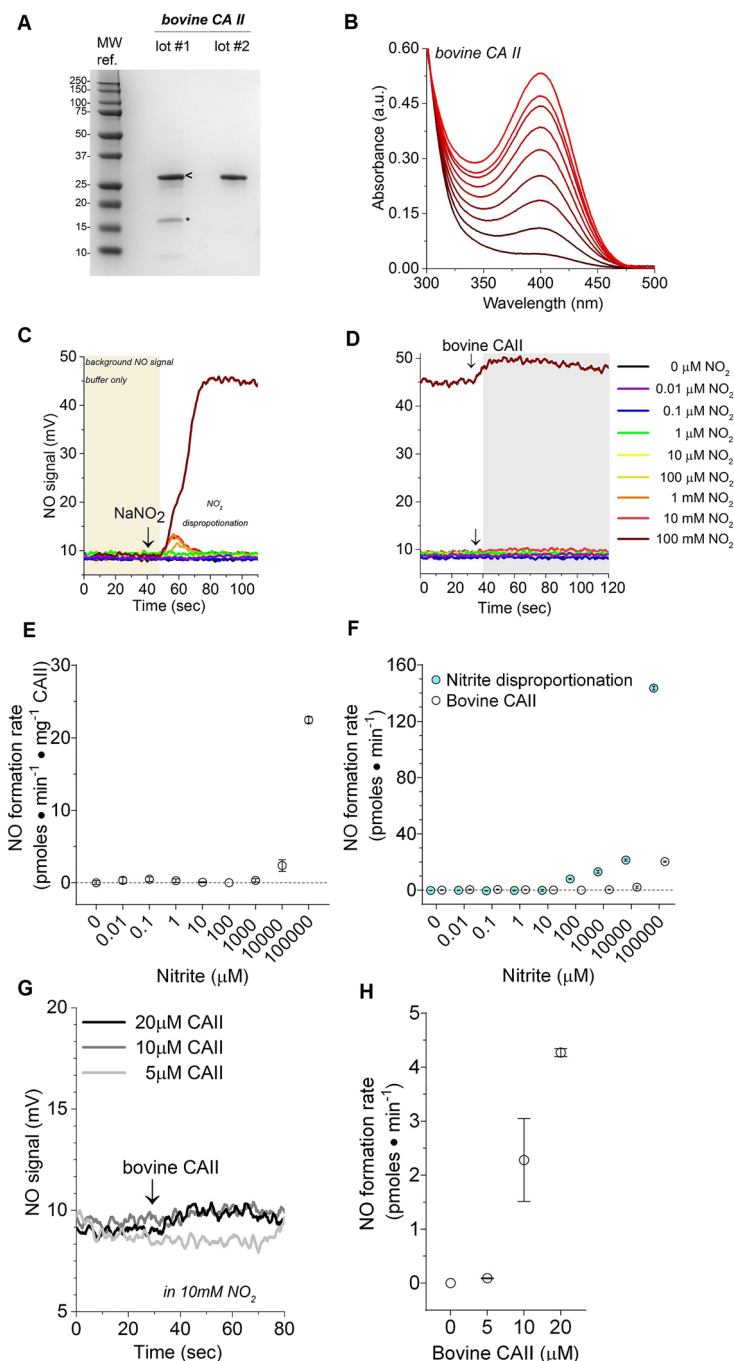


FIGURE 1 Isolated bovine CAII enzyme characterization and reactivity with nitrite. (a) Bovine CAII purity visualized with Coomassie blue stained SDS-PAGE. Two unique lots (labelled lot #1 and lot #2) of commercially available CAII (isolated from bovine erythrocytes) were investigated. Both lots contain a prominent 29 kDa band in agreement with the expected size of bovine CAII. However, low MW impurities are visible in lot #1. The bands in lot #1 labelled with “<” and “*” were analysed with MS. All enzymatic data presented in Figure 1b-g were collected with the purified lot #2. Details on lot #1 are included in the Figure S1. (b) Bovine CAII *p*-nitrophenyl acetate (*p*-NPA) hydrolysis activity assay. The hydrolysis assays were conducted in 50-mM phosphate buffer with 400-μM 4-NPA at 25°C and pH 7.5 using 3-μM bovine CAII. The product of *p*-NPA hydrolysis, *p*-nitrophenyl acetate (*p*-NP), has a characteristic absorbance at 405 nm. Accumulation of the *p*-NP was monitored over 5 min, after the addition of bovine CAII. Background *p*-NPA hydrolyses rates were collected for each reaction prior to the addition of enzyme and then subtracted from the measured enzymic rate. Isolated recombinant human CAII *p*-NPA hydrolysis activity assay. (c) Representative raw data illustrating the effect of a range of nitrite concentrations (10-nM to 100-mM final concentration) on NO chemiluminescence. In each reaction, 20 μl of sodium nitrite was injected into the liquid reaction (purge) vessel of a Sievers 280i NO analyser (NOA), and then the NO signal was recorded. (d) Representative raw data obtained after the injection of 30-μl bovine CAII (10 μM, final concentration) into the vessel with sodium nitrite. (e) Calculated NO-production rates measured from the reaction of bovine CAII and nitrite. (f) Comparison of NO-formation catalysed by bovine CAII and non-enzymatic nitrite disproportionation. (g) The effect of 5-, 10-, and 20-μM bovine CAII on NO-production rates using nitrite as substrate. (h) Summary of the data presented in panel (g). Data are shown as mean ± SD, *n* = 3 collected from each independent protein lot

PHARMACOLOGY (Harding et al., 2018), and are permanently archived in the Concise Guide to PHARMACOLOGY 2019/20 (Alexander et al., 2019).

3 | RESULTS

3.1 | NO formation from bovine CAII

The bovine CAII protein was first purified using IMAC to remove trace contaminants (e.g., free metals and haemoglobin). Purity of the isolated bovine CAII was assessed using protein electrophoresis (SDS-PAGE) and then stained with Coomassie blue to visualize protein bands (Figure 1a). We observed a strong band at approximately 29 kDa, consistent with the expected MW of bovine CAII. Next, catalytic competency was measured using the *p*-NPA hydrolysis assay (Figure 1b). The bovine CAII preparation produced approximately 20 moles of *p*-nitrophenol per second per mg protein.

The ability of bovine CAII to catalyse conversion of nitrite to NO was measured using NO photolysis-chemiluminescence. The rate of nitrite disproportionation to NO (Figure 1c) was recorded prior to the addition of enzyme to the reaction vessel (Figure 1d). The rate of NO production generated from nitrite disproportionation (Figure 1c) was subtracted from the enzymatic NO-production rate (Figure 1d) to obtain the rate of CAII catalysed NO production (Figure 1e) at various nitrite concentrations ranging from 10-pM to 100-mM sodium nitrite. It is important to note that the rate of NO disproportionation was much greater than that of the corrected CAII catalysed NO production rate (Figure 1f). Modulating bovine CAII concentration did not increase NO-formation rates significantly (Figure 1g,h).

It should be noted that some preparations of commercially available bovine CAII exhibited limited reactivity when the lyophilized protein was used without prior chromatographic separation (Figure S1). However, the calculated K_M , K_{cat} , and V_{max} values were very low compared with established mammalian nitrite reductases. These

preparations exhibited a faint pink colour in the protein solution after resuspension in phosphate buffer. The coloured protein solution was unexpected (Figure S1F), because zinc enzymes are colorless and the well characterized CAII enzyme does not contain iron or any pigments that could generate a red or pink colour. UV-VIS spectroscopy (Figure S1E) revealed a spectra consistent with oxyhemoglobin contamination. Additionally, MS confirmed the presence of distinct haemoglobin α and β chains in some of these preparations of commercially available bovine CAII. Therefore, the bovine CAII was re-isolated using IMAC, to decrease the presence of possible redox active contaminants that can reduce nitrite to form NO. As shown in Figure 1, the NO formation was eliminated with this purification, while the catalytic competency measured using the *p*-NPA hydrolysis assay was sustained.

3.2 | NO formation from human recombinant CAII

To test the reaction of CAII and nitrite, the full-length recombinant human CAII enzyme was prepared and isolated using standard chromatographic techniques. The human CAII bacterial expression plasmid was prepared according to published protocols (Fisher et al., 2005). Active wild-type human CAII was isolated from *E. coli* strain SoluBL21 using established methodologies (Banerjee et al., 2004). The human CAII was electrophoretically pure (Figure 2a) and catalytically competent, as demonstrated by the established *p*-NPA hydrolysis CA assay (Figure 2b). After establishing that the recombinant human CAII was active using the accepted *p*-NPA hydrolysis activity assay (Figure 2b), we determined the ability of human CAII to catalyse conversion of nitrite to NO using NO photolysis-chemiluminescence. However, the human CAII had no detectable NO-formation activity in the presence of nitrite (Figure 2c), in line with the bovine CAII data. Taken together, these studies suggest that CAII does not catalyse nitrite-dependent NO production, and a contaminant in some bovine CAII preparations may explain discordant findings as suggested by Andring et al. (2018) and Hanff et al. (2016).

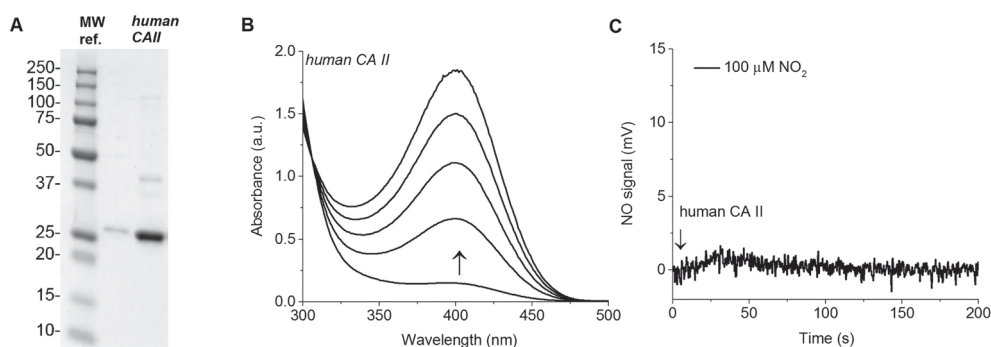


FIGURE 2 Isolated recombinant human CAII enzyme characterization and reactivity with nitrite. (a) Human CAII purity visualized with Coomassie blue stained SDS-PAGE. The three lanes include MW (MW ref.), dilute human CAII, and concentrated human CAII respectively. A roughly 29-kDa band is prominent in both human CAII lanes, in agreement with the expected size of recombinant human CAII. (b) The *p*-NPA hydrolysis activity assay conducted in 50-mM phosphate buffer with 400- μ M 4-NPA at 25°C and pH 7.5 using 1- μ M human CAII. (c) Raw data obtained by the measurement of NO using chemiluminescence during the reaction of human CAII and nitrite

3.3 | Levels of CAII in knockout mice

The availability of CAII knockout (KO) mice provides a tool to evaluate the function of CAII as a nitrite-dependent NOS *in vivo*. Mice lacking CAII display lower body weight, renal tubular acidosis, metabolic acidosis, respiratory acidosis, impaired urine acidification, and osteopetrosis (Lien & Lai, 1998; Shah, Bonapace, Hu, Strisciuglio, & Sly, 2004). The presence of CAII in various mouse tissues was determined by Western blotting analysis. In wild-type mice, CAII protein was detected in the liver, kidney, heart, lung (Figure 3a),

aorta (Figure 3b), and red blood cell ghosts (Figure 3c). As expected, CAII was not detectable in any tissues of the homozygous CAII^{-/-} mice. There was lower CAII expression in heterozygous CAII^{+/-} mice compared to wild-type mice. The complete depletion of CAII protein in CAII^{-/-} mice allows us to characterize the function of CAII in nitrite signalling in this model. Nitrite levels in urine and plasma were also measured to determine if CAII KO affects basal nitrite levels. No significant changes in urinary and plasma nitrite levels were detected between CAII^{-/-}, CAII^{+/-}, and wild-type mice (Figure S2).

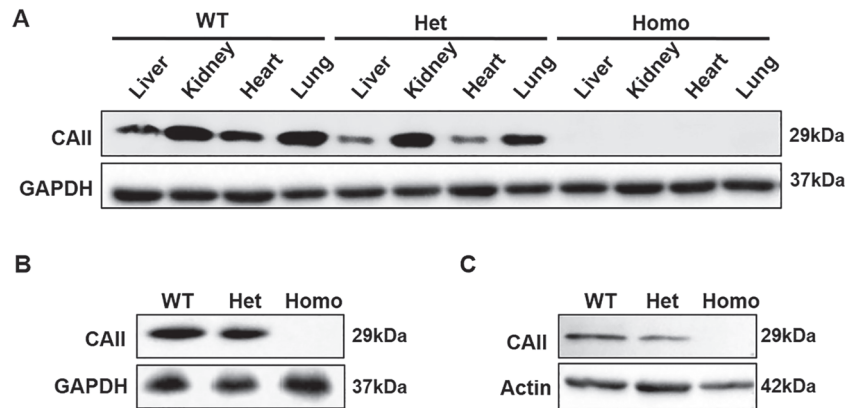


FIGURE 3 Deficiency of CAII protein in CAII knockout mice detected by Western blotting. (a) Detection of CAII protein in the liver, kidney, heart, and lung tissue homogenates from wild type (WT, CAII^{+/+}), heterozygous (Het, CAII^{+/-}), or homozygous (Homo, CAII^{-/-}) knockout mice. (b) Detection of CAII protein in aortic tissue homogenates. (c) Detection of CAII protein in red blood cell ghosts

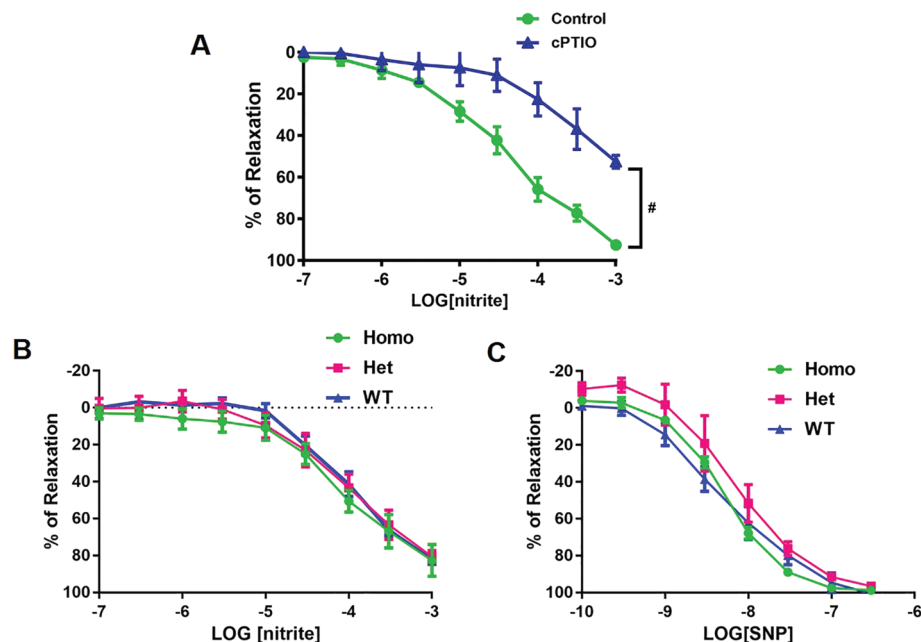


FIGURE 4 Concentration response curves to sodium nitrite and sodium nitroprusside (SNP) treatment in isolated aortas. (a) Concentration response curves of wild-type aortas ($n = 5$) to sodium nitrite in the presence of the NO scavenger, c-PTIO; # $P < .05$, significantly different from control. (b) Concentration response curves of CAII^{-/-}, CAII^{+/-}, and wild-type aortas ($n = 5$) to sodium nitrite. (c) Concentration response curves of CAII^{-/-}, CAII^{+/-}, and wild-type aortas ($n = 5$) to SNP. Values are shown as means \pm SEM and are expressed as the percentage of the maximal relaxation to phenylephrine (100 nM)

3.4 | CAII does not mediate nitrite-dependent vasodilation in aortic rings

Nitrite induced concentration-dependent relaxation of isolated wild-type aortic rings, which was significantly inhibited by pre-incubation with the specific NO scavenger, 2-(4-carboxyphenyl)-4,4,5,5-tetramethylimidazole-1-oxyl-3-oxide (c-PTIO, Figure 4a), indicating that NO formation contributes to nitrite-induced vessel relaxation. To assess whether aortic CAII plays a major role in nitrite-dependent vasodilation, aortas from CAII^{-/-} mice were compared with CAII^{+/-} and wild-type controls. No differences were observed in the response to nitrite among the aortas from CAII^{-/-}, CAII^{+/-}, and wild-type mice, suggesting that CAII does not mediate vascular NO production from nitrite (Figure 4b). Furthermore, there were no significant differences in NO donor SNP-induced relaxation among the

aortas from homozygous CAII^{-/-}, heterozygous CAII^{+/-}, and wild-type mice as well (Figure 4c).

3.5 | Erythrocytic CAII does not mediate the inhibition of platelet activation by nitrite

To further assess the role of erythrocytic CAII in nitrite-dependent NO production, we performed platelet activation assays in the presence of red blood cells isolated from CAII^{-/-}, CAII^{+/-}, and wild-type mice. We and others have reported that nitrite generates NO and inhibits platelet activation in the presence of red blood cells, which requires partial deoxygenation (Corti et al., 2016; Liu et al., 2015; Srihirun et al., 2012; Wang et al., 2006). Consistent with these data, we found that nitrite (10 μ M) significantly reduced platelet activation

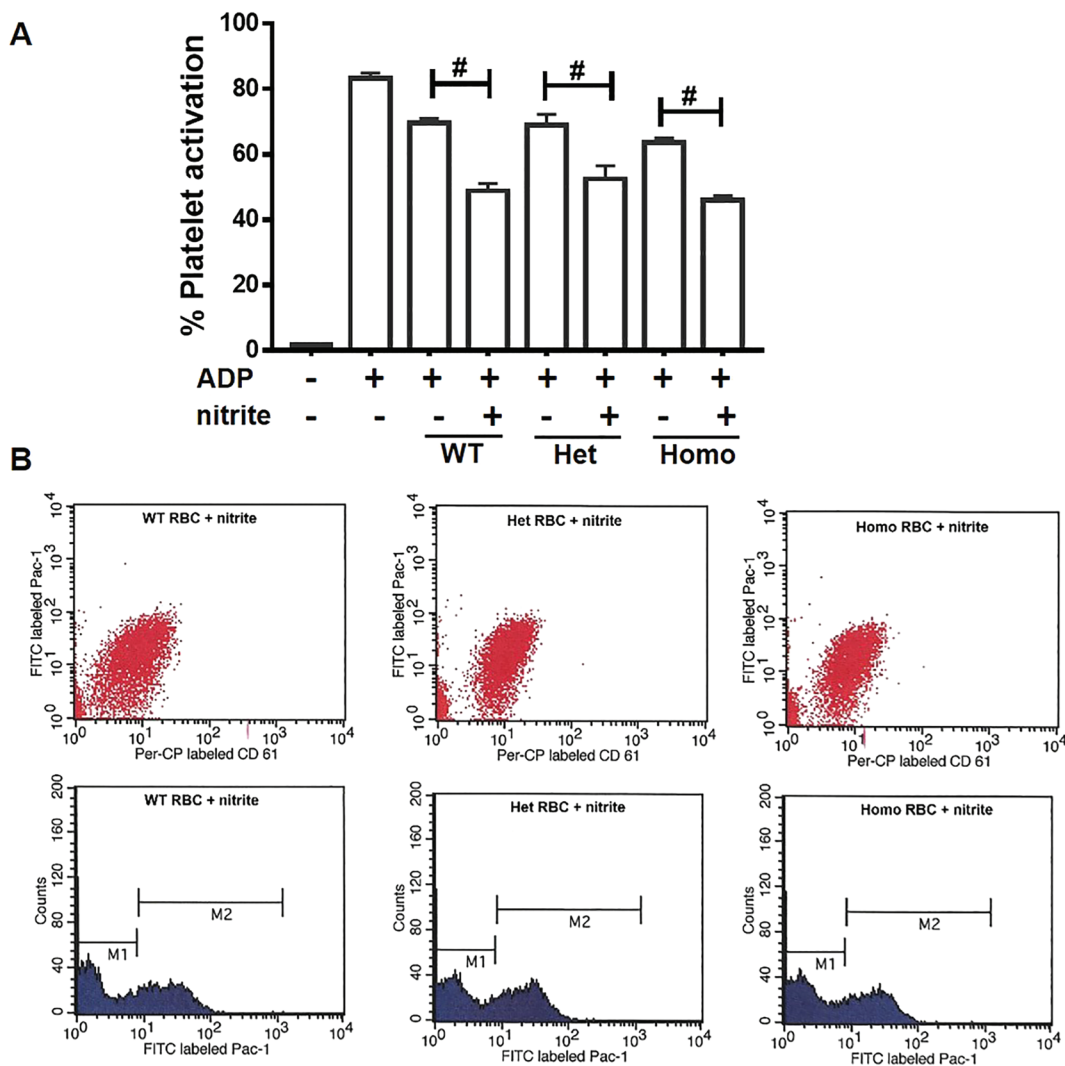


FIGURE 5 Carbonic anhydrase II does not affect erythrocytic nitrite-mediated platelet activation. Nitrite (10 μ M) was added to platelet rich plasma (PRP) and deoxygenated RBC (15% Hct) and allowed to incubate for 5 min before platelets were activated by ADP at 37°C. (a). Platelet activation assay presented in terms of % of activated platelets (PAC-1 positive events) in total platelets (CD61 positive events). (b) Flow cytometry detection of platelets treated with nitrite together with RBCs (80% deoxygenated). M1, population of non-activated platelets; M2, population of activated platelets. No significant differences were found among WT, Het, and KO RBCs. Data are presented as mean \pm SEM ($n = 8$ per group). # $P < .05$, significantly different as indicated

at pH 7.4 in the presence of deoxygenated wild-type red blood cells. However, in the presence of CAII^{-/-} red blood cells, nitrite inhibited platelet activation as well. No significant differences were found in the presence of RBCs from CAII^{-/-}, CAII^{+/-}, and wild-type mice (Figure 5).

3.6 | CAII does not modulate nitrite-induced blood pressure effects in vivo

To further investigate the role of NO formation from nitrite mediated by RBCs and vessel wall in regulating vascular tone in vivo, the effect of nitrite on blood pressure and heart rate was studied in anaesthetized mice. Nitrite infusion induced a significant dose-related decrease in arterial blood pressure in mice. However, CAII deletion in mice did not alter nitrite-dependent decreases in blood pressure (Figure 6). No significant differences were found in the response to nitrite among CAII^{-/-}, CAII^{+/-}, and wild-type mice.

4 | DISCUSSION

The role of CAII in nitrite-dependent NO production and vascular responses is controversial with conflicting published reports (Aamand et al., 2009a; Andring et al., 2018; Hanff et al., 2016; Pickerodt et al., 2018). Previous investigations utilized a combination of NO chemiluminescence, NO specific microelectrode, stable-isotope MS, and vascular myography to investigate the role of mammalian CAII catalysing the conversion of nitrite to NO. In this paper, the role of CAII in nitrite-dependent NO production was evaluated using enzyme kinetics, vascular myography, and CAII KO mice. We also revisited kinetics experiments with bovine CAII using NO chemiluminescence and presented new data using recombinant human CAII enzyme.

In our studies, both human recombinant and purified bovine CAII enzymes failed to catalyse nitrite reduction to NO, despite established

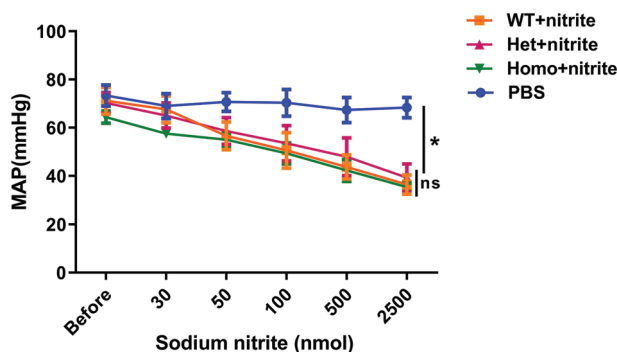


FIGURE 6 Mean arterial blood pressure changes respond to sodium nitrite infusion in CAII^{-/-}, CAII^{+/-}, and wild-type mice. Mice were infused with various doses of sodium nitrite. No significant differences were found among Homo (CAII^{-/-}), Het (CAII^{+/-}), and wild-type (WT) mice ($n = 6$). Values are shown as means \pm SEM. * $P < .05$, significantly different from PBS group; ns, not significantly different

p-NPA hydrolysis activity. Varying nitrite concentrations and bovine CAII enzyme concentrations failed to generate NO in a dose-dependent manner (Figure 1). However, we found that some lots of commercially available bovine CAII enzyme exhibited some reactivity with nitrite (Figure S1). Therefore, to determine whether the reactivity was due to a contaminate, the lyophilized powder was subjected to additional chromatographic processing. It was found that the “re-purified” bovine CAII had no nitrite reactivity but retained hydrolysis activity (Figure 1). MS identified distinct peptides from haemoglobin, a known nitrite reductase, in the reconstituted lyophilized bovine CAII samples, which were also confirmed by detection of haem Soret and Q-band spectra using UV-VIS spectroscopy. The presence of haemoglobin in the bovine erythrocyte CAII was not surprising, as CAII and haemoglobin are two of the most abundant enzymes in erythrocytes. It is important to note that Andring et al. (2018) who purified bovine CAII in-house with a modified protocol to eliminate possible contaminating material, such as haemoglobin or trace iron, did not find any NO production using NO-electrode, from bovine CAII, while the Aamand study utilized commercially available bovine erythrocyte CAII (also from Sigma) and, using NO-electrode, did observe NO production. Taken together, the data in Figure 1 suggest that the bovine CAII NO-formation represents an artefact of erythrocyte CAII isolation procedures and that CAII is not a nitrite-dependent NOS.

Moreover, the mechanism for how [dorzolamide](#), a well-established CA inhibitor, would increase NO-formation remains unclear and was not reproduced in our work or others (Andring et al., 2018; Hanff et al., 2016; Liu et al., 2015). Previously, CAII inhibitors, such as dorzolamide, were shown to paradoxically increase NO production from nitrite and bovine CAII using a NO-specific electrode by Aamand et al. (2009a), although no clear mechanism for this was established. However, we found no effect of dorzolamide on NO-production using NO chemiluminescence (data not included), in line with recent other reports (Andring et al., 2018; Hanff et al., 2016). The mechanism of CAII inhibition by dorzolamide has been well characterized, and structural data illustrate that dorzolamide and related inhibitors bind directly to the zinc in the active site of CAII (Pinard, Boone, Rife, Supuran, & McKenna, 2013). Additionally, nitrite is an established CAII inhibitor which is thought to bind to zinc directly, blocking carbon dioxide hydration and bicarbonate dehydration (Innocenti, Lehtonen, Parkkila, Scozzafava, & Supuran, 2004; Nielsen & Fago, 2015; Nishimori et al., 2009). A recent structural investigation concluded that nitrite and dorzolamide were unlikely to simultaneously bind to a single zinc atom in the CAII active site (Andring et al., 2018). As the original report (Aamand et al., 2009b) utilized NO electrode for NO detection, it is possible that they experienced an artefact of the NO electrode, which has less specificity than the NO chemiluminescence method or membrane inlet MS (Mikulski, Tu, Swenson, & Silverman, 2010).

Aamand et al. (2009b) were the first to report that a non-redox active metal (Zn^{2+}) could catalyse the transformation of nitrite to NO. While the zinc metal-binding active site of human CAII does share structural similarities to bacterial copper nitrite reductase (Cu-NiR; Strange et al., 1995), with three histidine residues cradelling the metal

atom in the enzyme active site, the active site is not completely conserved as the fourth histidine residue present in Cu-NiR is absent in CAII (Strange et al., 1999). Additionally, innate differences in electron configuration among the copper and zinc metal atoms render it unlikely that CAII and NiR share similar enzymatic mechanisms, as the redox active copper in NiR cycles between +2 and +1 oxidation states (Lindsog, 1997) while zinc in CAII is a Lewis acid and not redox active. The electronic differences among active site metals would override the similar first coordination sphere amino acid content (histidine) and the geometry of the substrate (nitrite and bicarbonate are both trigonal planar molecules).

There are 13 known, active mammalian CA isozymes, which differ in tissue distribution, subcellular locations (Supuran, 2008). CAII, the cytoplasmic isozyme, is one of the most widespread of the CA isozymes and also the one with the highest catalytic activity (Shah et al., 2004). The reaction of CAII and its native substrate CO_2 is one of the fastest characterized enzymatic reactions and is diffusion limited (Eriksson, Jones, & Liljas, 1988). Consistent with its function in ion regulation and in intracellular and extracellular acid-base homeostasis, CAII is expressed abundantly in a number of epithelial cells (Spicer, Sens, Hennigar, & Stoward, 1984) and red blood cells (Swenson & Maren, 1978). CAII is also expressed in variety of other cell types in different tissues, including the vasculature. In isolated bovine aortic smooth muscle, which is devoid of erythrocytes, CA is present in low concentrations, and roughly 75% of the CA activity is accounted for by CAI, with 20% due to CAII (Berg, Ramanathan, Gabrielli, & Swenson, 2004). In our study, mouse CAII protein was detected in the liver, kidney, heart, and lung as well as aorta and red blood cells in wild-type mice (Figure 3), which was completely depleted in CAII^{-/-} mice. As CA inhibitors may have unknown off-target effects due to different tissue specific isozymes expression (Swenson, 2016), the CAII deficient mouse model allowed us to characterize the function of CAII in nitrite signalling, on a relatively clean background. Although renal carbonic anhydrases (CAII and CAIV) are involved in the reabsorption of endogenous nitrite (Chobanyan-Jürgens et al., 2012; Zinke et al., 2016), we examined the effect of CAII KO on endogenous nitrite levels in urine and no differences were detected among CAII^{-/-}, CAII^{+/-}, and wild-type mice. Our assessment of levels of plasma nitrite support this finding with similar nitrite levels across the genotypes (Figure S2).

Pharmacological concentrations of exogenous nitrite relax pre-constricted isolated vessels and function as a more potent vasodilator under mild hypoxic or acidic conditions and in the human circulation (Cosby et al., 2003; Maher et al., 2008). However, our study did not find significant difference of nitrite-dependent vasodilation in isolated aorta rings (Figure 4) and in intact animals (Figure 6) among CAII^{-/-}, CAII^{+/-}, and wild-type mice, suggesting that CAII does not mediate NO formation from nitrite in the mouse circulation. It is important to point out that CAII-deficient mice have a mixed respiratory and metabolic acidosis (Lien & Lai, 1998) which may potentiate nitrite-dependent vasodilation in vivo. Despite the fact that CAII is expressed abundantly in red blood cells, we found that CAII KO red blood cells exhibited similar nitrite-dependent platelet inhibition compared with

wild-type red blood cells (Figure 5). Recently, Hanff et al. (2016) reported that nitrite and CAII can generate S-nitrosothiols (RSNOs) in the presence of cysteine, but we did not observe in vivo or in vitro vasodilation with CAII KO (Figures 4 and 6). While RSNOs are potent vasodilators, our observation suggests that this chemistry is not occurring in vivo. Our current finding that deletion of CAII gene did not affect the effects of nitrite on platelet activation and vasodilation provides further evidence that CAII is not responsible for nitrite bio-activation in red blood cells, vessel walls, and circulation. Moreover, inhibition of erythrocytic CAII by its inhibitor, dorzolamide, had no significant effect on NO production from RBCs, which further excludes the role of CAII and supports that deoxygenated haemoglobin within red blood cells is the main erythrocytic protein responsible for mediating nitrite-dependent NO signalling (Liu et al., 2015; Wajih et al., 2019). It should be noted that CAII inhibitors are used in a wide variety of clinical conditions to treat hypertension-related diseases (Swenson, 2014), which is incompatible with the role of CAII mediating NO formation as well.

In summary, the current study failed to validate the possibility that CAII catalysed the formation of NO from nitrite, in vitro or in vivo. Our findings demonstrate that CAII is not the enzyme responsible for the bio-activation of nitrite in the circulation. This is in agreement with other reports that CAII did not contribute to NO formation from nitrite reduction (Andring et al., 2018; Liu et al., 2015; Pickerodt et al., 2018). Further studies should explore other potential nitrite reductases which may have physiological significance in blood flow regulation. Elucidation of the pathway of nitrite mediated NO production will provide critical information about potential molecular targets for the development of new therapeutic agents to regulate vascular function.

ACKNOWLEDGEMENTS

This project used the UPCI Cancer Biomarkers Facility supported in part by award P30CA047904. The human CAII bacterial expression plasmid was a kind gift from David Silverman. M.T.G. receives research support from National Institutes of Health Grants 5R01HL098032-11, 2R01HL125886-05, 5P01HL103455-09, and 5T32HL110849-08, the Burroughs Wellcome Foundation, the Institute for Transfusion Medicine, and the Hemophilia Center of Western Pennsylvania. D.B.K-S. receives partial research support from National Institutes of Health grants 5R01HL098032-11 and 4R37HL058091-20. We thank Minying Yang for assistance with mice breeding and tissue collection.

AUTHOR CONTRIBUTIONS

M.T.G., L.W., and C.W. designed, conceived, and supervised the project. L.W. performed ex vivo and in vivo experiments, analysed the data and wrote the manuscript. C.W. conducted and supervised experiments with bovine and human CAII isolation, expression, and kinetic analysis, prepared figures, and wrote the manuscript. J.W. performed the initial biochemical investigations using the NO analyser and performed some of the *p*-NPA hydrolysis assays. N.W. conducted the platelet activation assay. P.V. conducted some

NO measurement experiments. Q.X. conducted animal surgery. E.C. assisted with NO measurements and SDS-PAGE analysis. J.T. assisted with experimental design and critical review and editing of the manuscript. M.S. assisted with project design and provided animal breeders. D.B.K-S. designed and supervised the platelet activation assay.

CONFLICTS OF INTEREST

M.T.G, Q.X., and J.T. are co-inventors of pending patent applications and planned patents directed to the use of recombinant neuroglobin and haem-based molecules as antidotes for carbon monoxide poisoning, which have been licensed by Globin Solutions, Inc. M.T.G. is a shareholder, advisor, and director in Globin Solutions, Inc. J.T. is a shareholder, advisor, and scientific chief officer in Globin Solutions, Inc. L.W. is a shareholder in Globin Solutions, Inc. M.T.G. and D.B.K-S. are co-inventors on patents directed to the use of nitrite salts in cardiovascular diseases, which were previously licensed to United Therapeutics and Hope Pharmaceuticals, and are now licensed to Globin Solutions, Inc. Additionally, M.T.G. is a co-investigator in a research collaboration with Bayer Pharmaceuticals to evaluate riociguat as a treatment for patients with sickle cell disease.

DECLARATION OF TRANSPARENCY AND SCIENTIFIC RIGOUR

This Declaration acknowledges that this paper adheres to the principles for transparent reporting and scientific rigour of preclinical research as stated in the *BJP* guidelines for [Design & Analysis](#), [Immunoblotting and Immunochemistry](#) and [Animal Experimentation](#), and as recommended by funding agencies, publishers and other organizations engaged with supporting research.

ORCID

Ling Wang  <https://orcid.org/0000-0003-4333-3158>

Courtney E. Sparacino-Watkins  <https://orcid.org/0000-0002-2954-9633>

Qinzi Xu  <https://orcid.org/0000-0002-3149-5777>

Jesús Tejero  <https://orcid.org/0000-0003-3245-9978>

Mark T. Gladwin  <https://orcid.org/0000-0001-7267-9006>

REFERENCES

- Aamand, R., Dalsgaard, T., Jensen, F. B., Simonsen, U., Roepstorff, A., & Fago, A. (2009a). Generation of nitric oxide from nitrite by carbonic anhydrase: A possible link between metabolic activity and vasodilation. *American Journal of Physiology - Heart and Circulatory Physiology*, 297, H2068–H2074.
- Aamand, R., Dalsgaard, T., Jensen, F. B., Simonsen, U., Roepstorff, A., & Fago, A. (2009b). Generation of nitric oxide from nitrite by carbonic anhydrase: A possible link between metabolic activity and vasodilation. *American Journal of Physiology. Heart and Circulatory Physiology*, 297, H2068–H2074.
- Alexander, S. P. H., Fabbro, D., Kelly, E., Mathie, A., Peters, J. A., Veale, E. L., ... CGTP Collaborators (2019). The Concise Guide to PHARMACOLOGY 2019/20: Enzymes. *British Journal of Pharmacology*, 176, S297–S396. <https://doi.org/10.1111/bph.14752>
- Alexander, S. P. H., Roberts, R. E., Broughton, B. R. S., Sobey, C. G., George, C. H., Stanford, S. C., ... Ahluwalia, A. (2018). Goals and practicalities of immunoblotting and immunohistochemistry: A guide for submission to the *British Journal of Pharmacology*. *British Journal of Pharmacology*, 175, 407–411.
- Andring, J. T., Lomelino, C. L., Tu, C., Silverman, D. N., McKenna, R., & Swenson, E. R. (2018). Carbonic anhydrase II does not exhibit nitrate reductase or nitrous anhydrase activity. *Free Radical Biology & Medicine*, 117, 1–5.
- Banerjee, A. L., Swanson, M., Mallik, S., & Srivastava, D. (2004). Purification of recombinant human carbonic anhydrase-II by metal affinity chromatography without incorporating histidine tags. *Protein Expression and Purification*, 37, 450–454.
- Basu, S., Grubina, R., Huang, J., Conradie, J., Huang, Z., Jeffers, A., ... Kim-Shapiro, D. B. (2007). Catalytic generation of N₂O₃ by the concerted nitrite reductase and anhydrase activity of hemoglobin. *Nature Chemical Biology*, 3, 785–794.
- Berg, J. T., Ramanathan, S., Gabrielli, M. G., & Swenson, E. R. (2004). Carbonic anhydrase in mammalian vascular smooth muscle. *The Journal of Histochemistry and Cytochemistry*, 52, 1101–1106.
- Chobanyan-Jürgens, K., Schwarz, A., Böhmer, A., Beckmann, B., Gutzki, F.-M., Michaelsen, J. T., ... Tsikas, D. (2012). Renal carbonic anhydrases are involved in the reabsorption of endogenous nitrite. *Nitric Oxide*, 26, 126–131.
- Corti, P., Xue, J., Tejero, J., Wajih, N., Sun, M., Stolz, D. B., ... Gladwin, M. T. (2016). Globin X is a six-coordinate globin that reduces nitrite to nitric oxide in fish red blood cells. *Proceedings of the National Academy of Sciences of the United States of America*, 113, 8538–8543.
- Cosby, K., Partovi, K. S., Crawford, J. H., Patel, R. P., Reiter, C. D., Martyr, S., ... Gladwin, M. T. (2003). Nitrite reduction to nitric oxide by deoxyhemoglobin vasodilates the human circulation. *Nature Medicine*, 9, 1498–1505.
- Curtis, M. J., Alexander, S., Cirino, G., Docherty, J. R., George, C. H., Giembycz, M. A., ... Ahluwalia, A. (2018). Experimental design and analysis and their reporting II: Updated and simplified guidance for authors and peer reviewers. *British Journal of Pharmacology*, 175, 987–993.
- Eriksson, A. E., Jones, T. A., & Liljas, A. (1988). Refined structure of human carbonic anhydrase II at 2.0 Å resolution. *Proteins: Structure, Function, and Bioinformatics*, 4, 274–282.
- Fisher, Z., Hernandez Prada, J. A., Tu, C., Duda, D., Yoshioka, C., An, H., ... McKenna, R. (2005). Structural and kinetic characterization of active-site histidine as a proton shuttle in catalysis by human carbonic anhydrase II. *Biochemistry*, 44, 1097–1105.
- Gladwin, M. T., Raat, N. J., Shiva, S., Dezfulian, C., Hogg, N., Kim-Shapiro, D. B., & Patel, R. P. (2006). Nitrite as a vascular endocrine nitric oxide reservoir that contributes to hypoxic signaling, cytoprotection, and vasodilation. *American Journal of Physiology. Heart and Circulatory Physiology*, 291, H2026–H2035.
- Hanff, E., Böhmer, A., Zinke, M., Gambaryan, S., Schwarz, A., Supuran, C. T., & Tsikas, D. (2016). Carbonic anhydrases are producers of S-nitrosothiols from inorganic nitrite and modulators of soluble guanylyl cyclase in human platelets. *Amino Acids*, 48, 1695–1706.
- Hanff, E., Zinke, M., Böhmer, A., Niebuhr, J., Maassen, M., Endeward, V., ... Tsikas, D. (2018). GC-MS determination of nitrous anhydrase activity of bovine and human carbonic anhydrase II and IV. *Analytical Biochemistry*, 550, 132–136.
- Harding, S. D., Sharman, J. L., Faccenda, E., Southan, C., Pawson, A. J., Ireland, S., ... NC-IUPHAR. (2018). The IUPHAR/BPS Guide to PHARMACOLOGY in 2018: Updates and expansion to encompass the new guide to IMMUNOPHARMACOLOGY. *Nucleic Acids Research*, 46, D1091–D1106.

- He, C., & Knipp, M. (2009). Formation of nitric oxide from nitrite by the ferriheme b protein nitrophorin 7. *Journal of the American Chemical Society*, 131, 12042–12043.
- Huang, Z., Shiva, S., Kim-Shapiro, D. B., Patel, R. P., Ringwood, L. A., Irby, C. E., ... Gladwin, M. T. (2005). Enzymatic function of hemoglobin as a nitrite reductase that produces NO under allosteric control. *The Journal of Clinical Investigation*, 115, 2099–2107.
- Innocenti, A., Lehtonen, J. M., Parkkila, S., Scozzafava, A., & Supuran, C. T. (2004). Carbonic anhydrase inhibitors. Inhibition of the newly isolated murine isozyme XIII with anions. *Bioorganic and Medicinal Chemistry Letters*, 14, 5435–5439.
- Innocenti, A., Zimmerman, S., Ferry, J. G., Scozzafava, A., & Supuran, C. T. (2004). Carbonic anhydrase inhibitors. Inhibition of the zinc and cobalt γ -class enzyme from the archaeon *Methanosarcina thermophila* with anions. *Bioorganic & Medicinal Chemistry Letters*, 14, 3327–3331.
- Kilkenny, C., Browne, W., Cuthill, I. C., Emerson, M., & Altman, D. G. (2010). Animal research: Reporting *in vivo* experiments: the ARRIVE guidelines. *British Journal of Pharmacology*, 160, 1577–1579.
- Kim-Shapiro, D. B., & Gladwin, M. T. (2014). Mechanisms of nitrite bioactivation. *Nitric Oxide*, 38, 58–68.
- Lewis, S. E., Erickson, R. P., Barnett, L. B., Venta, P. J., & Tashian, R. E. (1988). N-ethyl-N-nitrosourea-induced null mutation at the mouse Car-2 locus: an animal model for human carbonic anhydrase II deficiency syndrome. *Proceedings of the National Academy of Sciences of the United States of America*, 85, 1962–1966.
- Li, H., Hemann, C., Abdelghany, T. M., El-Mahdy, M. A., & Zweier, J. L. (2012). Characterization of the mechanism and magnitude of cytoglobin-mediated nitrite reduction and nitric oxide generation under anaerobic conditions. *The Journal of Biological Chemistry*, 287, 36623–36633.
- Li, H., Kundu, T. K., & Zweier, J. L. (2009). Characterization of the magnitude and mechanism of aldehyde oxidase-mediated nitric oxide production from nitrite. *Journal of Biological Chemistry*, 284, 33850–33858.
- Li, H., Samouilov, A., Liu, X., & Zweier, J. L. (2001). Characterization of the magnitude and kinetics of xanthine oxidase-catalyzed nitrite reduction. Evaluation of its role in nitric oxide generation in anoxic tissues. *The Journal of Biological Chemistry*, 276, 24482–24489.
- Lien, Y. H., & Lai, L. W. (1998). Respiratory acidosis in carbonic anhydrase II-deficient mice. *The American Journal of Physiology*, 274, L301–L304.
- Lindskog, S. (1997). Structure and mechanism of carbonic anhydrase. *Pharmacology & Therapeutics*, 74, 1–20.
- Liu, C., Wajih, N., Liu, X., Basu, S., Janes, J., Marvel, M., ... Kim-Shapiro, D. B. (2015). Mechanisms of human erythrocytic bioactivation of nitrite. *The Journal of Biological Chemistry*, 290, 1281–1294.
- Lundberg, J. O., Gladwin, M. T., Ahluwalia, A., Benjamin, N., Bryan, N. S., Butler, A., ... Weitzberg, E. (2009). Nitrate and nitrite in biology, nutrition and therapeutics. *Nature Chemical Biology*, 5, 865–869.
- Lundberg, J. O., Weitzberg, E., & Gladwin, M. T. (2008). The nitrate-nitrite-nitric oxide pathway in physiology and therapeutics. *Nature Reviews. Drug Discovery*, 7, 156–167.
- MacArthur, P. H., Shiva, S., & Gladwin, M. T. (2007). Measurement of circulating nitrite and S-nitrosothiols by reductive chemiluminescence. *Journal of Chromatography B*, 851, 93–105.
- Maher, A. R., Milsom, A. B., Gunaruwan, P., Abozguia, K., Ahmed, I., Weaver, R. A., ... Frenneaux, M. P. (2008). Hypoxic modulation of exogenous nitrite-induced vasodilation in humans. *Circulation*, 117, 670–677.
- McGrath, J. C., & Lilley, E. (2015). Implementing guidelines on reporting research using animals (ARRIVE etc.): New requirements for publication in BJP. *British Journal of Pharmacology*, 172, 3189–3193.
- Mikulski, R., Tu, C., Swenson, E. R., & Silverman, D. N. (2010). Reactions of nitrite in erythrocyte suspensions measured by membrane inlet mass spectrometry. *Free Radical Biology & Medicine*, 48, 325–331.
- Nielsen, P. M., & Fago, A. (2015). Inhibitory effects of nitrite on the reactions of bovine carbonic anhydrase II with CO₂ and bicarbonate consistent with zinc-bound nitrite. *Journal of Inorganic Biochemistry*, 149, 6–11.
- Nishimori, I., Minakuchi, T., Onishi, S., Vullo, D., Cecchi, A., Scozzafava, A., & Supuran, C. T. (2009). Carbonic anhydrase inhibitors. Cloning, characterization and inhibition studies of the cytosolic isozyme III with anions. *Journal of Enzyme Inhibition and Medicinal Chemistry*, 24, 70–76.
- Pickeroth, P. A., Kronfeldt, S., Russ, M., Gonzalez-Lopez, A., Lothar, P., Steiner, E., ... Swenson, E. R. (2018). Carbonic anhydrase is not a relevant nitrite reductase or nitrous anhydrase in the lung. *The Journal of Physiology*, 597(4), 1045–1058.
- Pinard, M. A., Boone, C. D., Rife, B. D., Supuran, C. T., & McKenna, R. (2013). Structural study of interaction between brinzolamide and dorzolamide inhibition of human carbonic anhydrases. *Bioorganic & Medicinal Chemistry*, 21, 7210–7215.
- Pocker, Y., & Stone, J. (1967). The catalytic versatility of erythrocyte carbonic anhydrase. III. Kinetic studies of the enzyme-catalyzed hydrolysis of p-nitrophenyl acetate. *Biochemistry*, 6, 668–678.
- Shah, G. N., Bonapace, G., Hu, P. Y., Strisciuglio, P., & Sly, W. S. (2004). Carbonic anhydrase II deficiency syndrome (osteopetrosis with renal tubular acidosis and brain calcification): Novel mutations in CA2 identified by direct sequencing expand the opportunity for genotype-phenotype correlation. *Human Mutation*, 24, 272–272.
- Shevchenko, A., Tomas, H., Havlis, J., Olsen, J. V., & Mann, M. (2006). In-gel digestion for mass spectrometric characterization of proteins and proteomes. *Nature Protocols*, 1, 2856–2860.
- Shiva, S. (2013). Nitrite: A physiological store of nitric oxide and modulator of mitochondrial function. *Redox Biology*, 1, 40–44.
- Shiva, S., Huang, Z., Grubina, R., Sun, J., Ringwood, L. A., MacArthur, P. H., ... Gladwin, M. T. (2007). Deoxymyoglobin is a nitrite reductase that generates nitric oxide and regulates mitochondrial respiration. *Circulation Research*, 100, 654–661.
- Silverman, D. N., & Lindskog, S. (1988). The catalytic mechanism of carbonic anhydrase: Implications of a rate-limiting protolysis of water. *Accounts of Chemical Research*, 21, 30–36.
- Sparacino-Watkins, C. E., Tejero, J., Sun, B., Gauthier, M. C., Thomas, J., Ragireddy, V., ... Gladwin, M. T. (2014). Nitrite reductase and nitric oxide synthase activity of the mitochondrial molybdopterin enzymes mARC1 and mARC2. *The Journal of Biological Chemistry*, 289, 10345–10358.
- Spicer, S. S., Sens, M. A., Hennigar, R. A., & Stoward, P. J. (1984). Implications of the immunohistochemical localization of the carbonic anhydrase isozymes for their function in normal and pathologic cells. *Annals of the New York Academy of Sciences*, 429, 382–397.
- Srihirun, S., Sriwantana, T., Unchern, S., Kittikool, D., Nulsri, E., Pattanapanyasat, K., ... Sibmooch, N. (2012). Platelet inhibition by nitrite is dependent on erythrocytes and deoxygenation. *PLoS ONE*, 7, e30380.
- Strange, R. W., Murphy, L. M., Dodd, F. E., Abraham, Z. H., Eady, R. R., Smith, B. E., & Hasnain, S. S. (1999). Structural and kinetic evidence for an ordered mechanism of copper nitrite reductase. *Journal of Molecular Biology*, 287, 1001–1009.
- Strange, R. W. D. F., Abraham, Z. H., Grossmann, J. G., Brüser, T., Eady, R. R., Smith, B. E., & Hasnain, S. S. (1995). The substrate-binding site in Cu nitrite reductase and its similarity to Zn carbonic anhydrase. *Nature Structural Biology*, 4, 287–292.

- Supuran, C. T. (2008). Carbonic anhydrases: novel therapeutic applications for inhibitors and activators. *Nature Reviews. Drug Discovery*, 7, 168–181.
- Swenson, E. R. (2014). New insights into carbonic anhydrase inhibition, vasodilation, and treatment of hypertensive-related diseases. *Current Hypertension Reports*, 16, 467–477.
- Swenson, E. R. (2016, 1985). Pharmacology of acute mountain sickness: Old drugs and newer thinking. *Journal of Applied Physiology*, 120, 204–215.
- Swenson, E. R., & Maren, T. H. (1978). A quantitative analysis of CO₂ transport at rest and during maximal exercise. *Respiration Physiology*, 35, 129–159.
- Tiso, M., Tejero, J., Basu, S., Azarov, I., Wang, X., Simplaceanu, V., ... Gladwin, M. T. (2011). Human Neuroglobin Functions as a Redox-regulated Nitrite Reductase. *The Journal of Biological Chemistry*, 286, 18277–18289.
- Tu, C., Silverman, D. N., Forsman, C., Jonsson, B. H., & Lindskog, S. (1989). Role of histidine 64 in the catalytic mechanism of human carbonic anhydrase II studied with a site-specific mutant. *Biochemistry*, 28, 7913–7918.
- Wajih, N., Basu, S., Ucer, K. B., Rigal, F., Shakya, A., Rahbar, E., ... Shapiro, D. B. (2019). Erythrocytic bioactivation of nitrite and its potentiation by far-red light. *Redox Biology*, 20, 442–450.
- Wang, J., Krizowski, S., Fischer-Schrader, K., Niks, D., Tejero, J., Sparacino-Watkins, C., ... Gladwin, M. T. (2015). Sulfite oxidase catalyzes single-electron transfer at molybdenum domain to reduce nitrite to nitric oxide. *Antioxidants & Redox Signaling*, 23, 283–294.
- Wang, X., Bryan, N. S., MacArthur, P. H., Rodriguez, J., Gladwin, M. T., & Feelisch, M. (2006). Measurement of nitric oxide levels in the red cell: Validation of tri-iodide-based chemiluminescence with acid-sulfanilamide pretreatment. *The Journal of Biological Chemistry*, 281, 26994–27002.
- Zinke, M., Hanff, E., Böhmer, A., Supuran, C. T., & Tsikas, D. (2016). Discovery and microassay of a nitrite-dependent carbonic anhydrase activity by stable-isotope dilution gas chromatography-mass spectrometry. *Amino Acids*, 48, 245–255.

SUPPORTING INFORMATION

Additional supporting information may be found online in the Supporting Information section at the end of this article.

How to cite this article: Wang L, Sparacino-Watkins CE, Wang J, et al. Carbonic anhydrase II does not regulate nitrite-dependent nitric oxide formation and vasodilation. *Br J Pharmacol.* 2020;177:898–911. <https://doi.org/10.1111/bph.14887>